Membrane translocation of lumenal domains of membrane proteins powered by downstream transmembrane sequences

Takaaki Yabuki*, Fumiko Morimoto*, Yuichiro Kida, and Masao Sakaguchi
Graduate School of Life Science, University of Hyogo, 3-2-1 Kouto, Kamigori, Ako-gun, Hyogo 678-1297, Japan

ABSTRACT **Translocation of the N-terminus of a type I signal anchor (SA-I) sequence across the endoplasmic reticulum membrane can be arrested by tagging with a streptavidin-binding peptide tag (SBP tag) and trapping by streptavidin. In the present study, we first examine the affinity required for the translocation arrest. When the SBP tag is serially truncated, the ability for arrest gradually decreases. Surface plasmon resonance analysis shows that an interaction as strong as 10^{-8} M or a smaller dissociation constant is required for trapping the topogenesis of a natural SA-I sequence. Such truncated tags, however, become effective by mutating the SA-I sequence, suggesting that the translocation motivation is considerably influenced by the properties of the SA-I sequence. In addition, we introduce the SBP tag into lumenal loops of a multispanning membrane protein, human erythrocyte band 3. Among the tagged loops between transmembrane 1 (TM1) and TM8, three loops are trapped by cytosolic streptavidin. These loops are followed by TM sequences possessing topogenic properties, like the SA-I sequence, and translocation of one loop is diminished by insertion of a proline into the following TM sequence. These findings suggest that the translocation of lumenal loops by SA-I–like TM sequences has a crucial role in topogenesis of multispanning membrane proteins.**

Monitoring Editor
Reid Gilmore
University of Massachusetts

Received: Apr 22, 2013
Revised: Jul 17, 2013
Accepted: Jul 29, 2013

INTRODUCTION

Large numbers of integral membrane proteins are located in organelles on the secretory pathway and plasma membrane in eukaryotic cells. Most of these proteins are cotranslationally integrated into the endoplasmic reticulum (ER) membrane via a protein-conducting channel, the so-called translocon (Alder and Johnson, 2004; Shao and Hegde, 2011; Park and Rapoport, 2012). The Sec61 complex, comprising three membrane proteins—Sec61α, Sec61β, and Sec61γ—is the central channel of the translocon. Based on site-specific cross-linking analyses during cotranslational protein integration (Mothes *et al.*, 1994, 1997; Martoglio *et al.*, 1995; Do *et al.*, 1996; Heinrich *et al.*, 2000), partitioning of a transmembrane (TM) sequence into the lipid bilayer is also mediated by the Sec61 channel. Observation of three-dimensional structures of archaeal (Van den Berg *et al.*, 2004) and bacterial (Tsukazaki *et al.*, 2008) SecY complexes, which are homologues of the eukaryotic Sec61 complex, revealed that the SecY protein (and probably the Sec61α subunit) forms a lateral gate into the lipid environment, as well as an hourglass-shaped pore. Because the TM2 and TM7 of yeast Sec61, which face the lateral seam in SecY structures, are adjacent to a signal sequence (Plath *et al.*, 1998), it is believed that signal and TM sequences are transferred laterally through the seam to the lipid bilayer. Several reports described functions of the Sec61 translocon beyond translocation and integration. In the integration of multispanning membrane proteins, several TM sequences and/or translocating chains can be simultaneously associated with Sec61α (Heinrich and Rapoport, 2003; Sadlish *et al.*, 2005; Ismail *et al.*, 2006; Kida *et al.*, 2007, 2010), suggesting that the Sec61 channel

This article was published online ahead of print in MBoC in Press (http://www.molbiolcell.org/cgi/doi/10.1091/mbc.E13-04-0210) on August 7, 2013.

*These authors contributed equally to this work.

Address correspondence to: Yuichiro Kida (ykida@sci.u-hyogo.ac.jp), Masao Sakaguchi (sakag@sci.u-hyogo.ac.jp).

Abbreviations used: ER, endoplasmic reticulum; HRP, horseradish peroxidase; k_a, association rate constant; K_D, dissociation constant; k_d, dissociation rate constant; MBP, *Escherichia coli* maltose-binding protein; RM, rough microsomal membrane; SA-I, type I signal anchor; SAv, streptavidin; SBP tag, streptavidin-binding peptide tag; SPR, surface plasmon resonance; SytII, synaptotagmin II; TM, transmembrane.

forms a larger complex and/or acceptable environment for more than one translocating and integrating chain and may function in the folding of multispanning membrane proteins.

The biogenesis of membrane proteins begins with cotranslational targeting caused by their signal sequences. After recognition by the signal recognition particle and targeting to the ER membrane via the signal recognition particle receptor, signal sequences are inserted into the translocon by assuming their own orientations. Cleavable signal peptides and type II signal anchor sequences translocate the portions following them to the lumenal space and settle in an $N_{cytosol}/C_{lumen}$ orientation. On the other hand, type I signal anchor (SA-I) sequences form the $N_{lumen}/C_{cytosol}$ orientation. The topology of signal sequences is influenced mainly by the length, hydrophobicity, and difference in net charges of flanking regions (Sakaguchi, 1997; Goder and Spiess, 2001). Several SA-I sequences possess positively charged regions downstream of hydrophobic segments, and such positive charges are crucial for the translocation of N-terminal domains (Kida *et al.*, 2000, 2006). We previously reported the controlled translocation of the SA-I sequence: the N-terminal domain of the SA-I sequence of mouse synaptotagmin II (SytII) tagged with a streptavidin-binding peptide tag (SBP tag) sequence can be captured by streptavidin in the cytosol, resulting in translocation arrest (Kida *et al.*, 2007). Because trapping the translocation of the N-terminal domain causes retention of the hydrophobic core part of the SA-I sequence in an aqueous environment (Kida *et al.*, 2010), translocation is firmly coupled with the membrane integration of the SA-I sequence.

In the case of multispanning membrane proteins, the TM sequences after signal sequences are cotranslationally integrated one by one into the ER membrane. In the canonical mode, a TM sequence with the $N_{cytosol}/C_{lumen}$ orientation starts translocation of the following part, and the subsequent TM sequence in the translocating chain stops at the translocon and is partitioned into the membrane. Marginally hydrophobic TM sequences are found in multispanning membrane proteins, however, and such TM sequences possess only weak start- and/or stop-transfer function (Ota *et al.*, 1998a). Based on the findings from several studies (Lu *et al.*, 1998; Ota *et al.*, 1998b; Ojemalm *et al.*, 2012), low topogenic TM sequences can be integrated by support from the following TM sequences possessing high topogenic functions. In such cases, the upstream TM sequence and loop are believed to be retained in the cytoplasmic or lumenal space until the downstream TM sequence emerges and moves into the translocon.

In the present study, we investigate the translocation of lumenal domains of the SA-I sequence and a multispanning membrane protein band 3 using the SBP-tagging technique. On the basis of analyses using tags with different affinities to streptavidin, we find that either an interaction as strong as 10^{-8} M or a smaller dissociation constant (K_D) is required to trap the N-terminal domain followed by the natural SA-I sequence and that the affinity required for the trapping is influenced by the primary structure of the SA-I sequence. These findings may indicate kinetic differences of each SA-I sequence in topogenesis and integration. Further, several tagged lumenal loops of the band 3 protein are trapped by cytosolic streptavidin. The finding that translocation of such a loop is diminished by mutation in the following TM sequence possessing a topogenic function like the SA-I sequence suggested that translocation of lumenal loops induced by internal SA-I-like TM sequences functions in the integration of multispanning membrane proteins.

RESULTS

Strong interaction is required to trap the translocation of the SBP-tagged N-terminal domain of the SA-I sequence

By fusion of the SBP tag to the N-terminal domain of the SA-I sequence of SytII, translocation can be trapped by streptavidin on the cytosolic side (Kida *et al.*, 2007). We wondered how tight the binding needs to be for the arrest to occur. Because partial deletion of an SBP tag weakens its interaction with streptavidin (Wilson *et al.*, 2001), we analyzed the arrest abilities of serially deleted SBP tags (Figure 1A). SBP-SytII fusion proteins, which possess two Asn-linked glycosylation sites between the SBP tag and SA-I sequence, were synthesized in a cell-free system in the presence of rough microsomal membranes (RMs) and the indicated concentrations of streptavidin (Figure 1B). All proteins in Figure 1B were largely detected in their unglycosylated or diglycosylated forms, suggesting that both glycosylation sites are effective and that a translocation stall between those sites rarely occurs. In the case of protein containing a normal SBP tag, glycosylation was inhibited by a higher concentration of streptavidin (Figure 1, B, lanes 1–5, and C), as described previously (Kida *et al.*, 2009). When the tag sequence was gradually deleted, a four-residue-deleted SBP tag (Δ4) behaved similarly to the normal tag, whereas the inhibitory effect on translocation was diminished by further partial deletions of the SBP tag (Figure 1, B and C).

Insertion of a proline residue into the SA-I sequence weakens the translocation motive force affecting the N-terminal domain (Kida *et al.*, 2009). We applied the same mutation on the proteins containing deleted SBP tags (Figure 2A). The proline-inserted SA-I sequence had a slightly weaker but still efficient ability to translocate its upstream domain with the ineffective concentration of streptavidin (Figure 2, B, lanes 1, 6, 11, 16, 21, and 26, and C). Even largely deleted SBP tags, however, became effective in the translocation arrest by proline insertion into the SA-I sequence (Figure 2, B and C). For example, 0.1 mg/ml (~6 μM) streptavidin efficiently trapped only the translocation of normal and four-residue-deleted tags in the protein with a wild-type SA-I sequence (Figure 2D). In the case of a proline-inserted SA-I sequence, however, the same concentration of streptavidin was effective in trapping the eight-residue-deleted tag.

To determine the actual binding affinity between each tag and streptavidin, we analyzed their interaction by surface plasmon resonance (SPR). To this end, we constructed SBP-Syt40–*Escherichia coli* maltose-binding protein (MBP) fusion proteins comprising normal or deleted SBP tags, N-terminal 2–40 residues of SytII, and MBP (Figure 3A). These proteins were expressed in *E. coli* cells and purified from cell extracts by chromatography using amylose resin. Purified proteins could be detected by decorating with streptavidin–horseradish peroxidase (HRP), except for the protein species with the 18-residue-deleted tag (Figure 3A). Streptavidin was fixed on sensor chips, and its interaction with SBP-tagged proteins was analyzed by SPR (Figure 3, B and C). Original and four-residue-deleted tags revealed quite low K_D with streptavidin, consistent with their strong ability to arrest translocation. Tags with six to eight residues deleted showed K_D values one digit higher than original and four-residue-deleted tags, and deletion of 12 residues of the tag largely increased the K_D. The 18-residue-deleted tag showed the weakest binding, suggesting that this affinity is rather insufficient for translocation trapping and detection using streptavidin–HRP. According to the association and dissociation rate constants (k_a and k_d, respectively; Figure 3C), the order of the values of dissociation rate constant is well matched to the order of efficiency of translocation trapping.

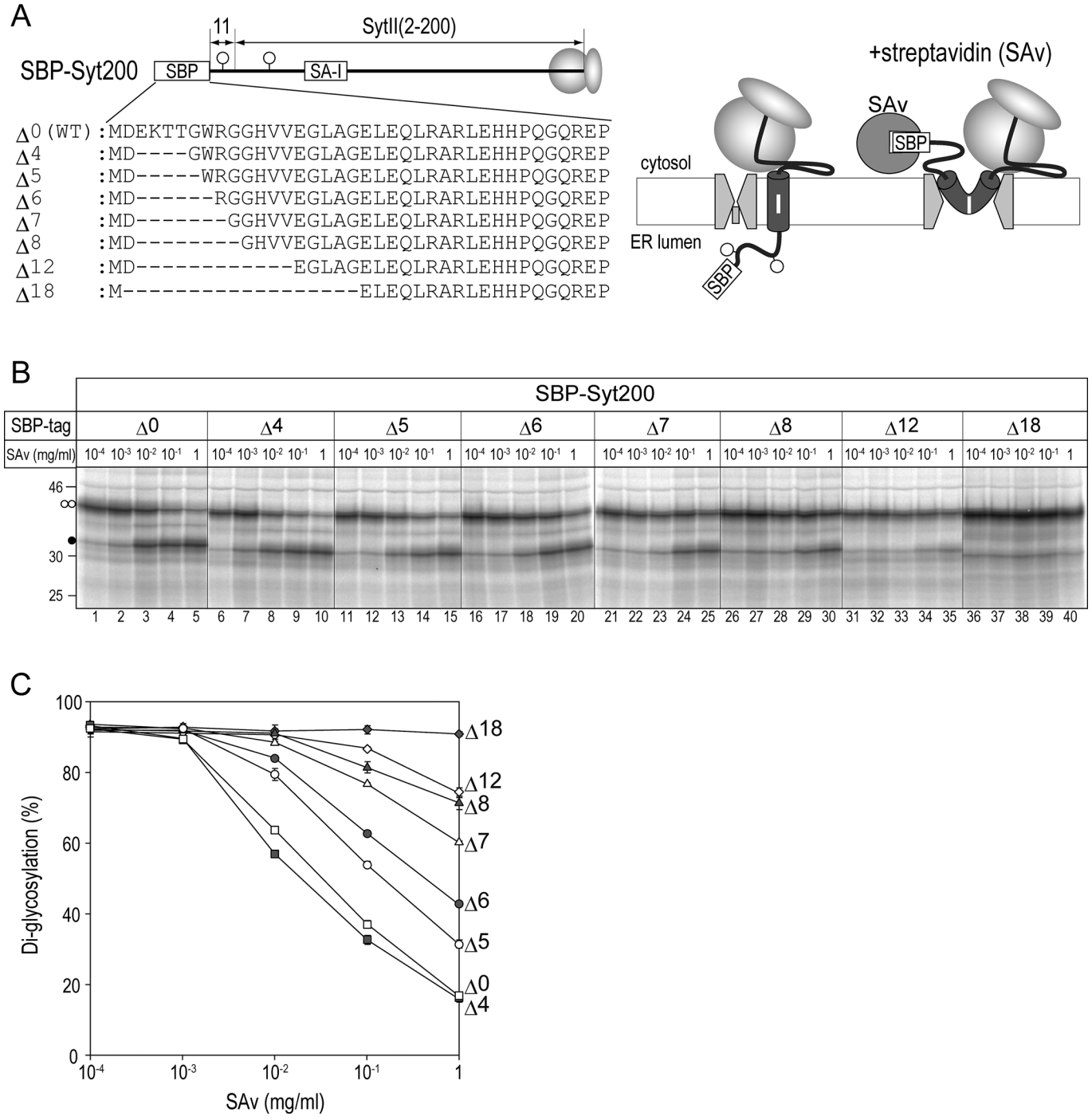

FIGURE 1: Trapping of the translocation of the N-terminal domain by truncated SBP tags. (A) SBP tag fused to the N-terminal domain of the SA-I sequence of SytII Arg-2–Arg-200 was serially deleted. Deleted residues are indicated by dashes. Two asparagine-linked glycosylation sites between the SBP tag and the SA-I sequence (open circles) were glycosylated when translocated into the ER lumen. If a truncated tag was effective, translocation of the tagged domain was trapped by streptavidin (SAv). (B) SBP-Syt200 fusion proteins containing full and truncated SBP tags were synthesized in vitro in the presence of RM and the indicated concentrations of SAv. After RM sedimentation, proteins included in RM were analyzed by SDS–PAGE. Closed circle and two open circles indicate unglycosylated and diglycosylated proteins, respectively. (C) Quantification of B. Diglycosylation efficiency of unglycosylated, monoglycosylated, and diglycosylated products in each lane was quantified. Mean value and SD of three independent experiments.

The foregoing results indicate that an interaction as strong as 10^{-8} M or a smaller K_D is required for trapping the translocation of the N-terminal domain caused by the SA-I sequence. The fact that the affinity required for translocation trapping was reduced by a proline insertion into the SA-I sequence indicates that the hydrophobic core of the SA-I sequence itself is deeply involved in the translocation motion.

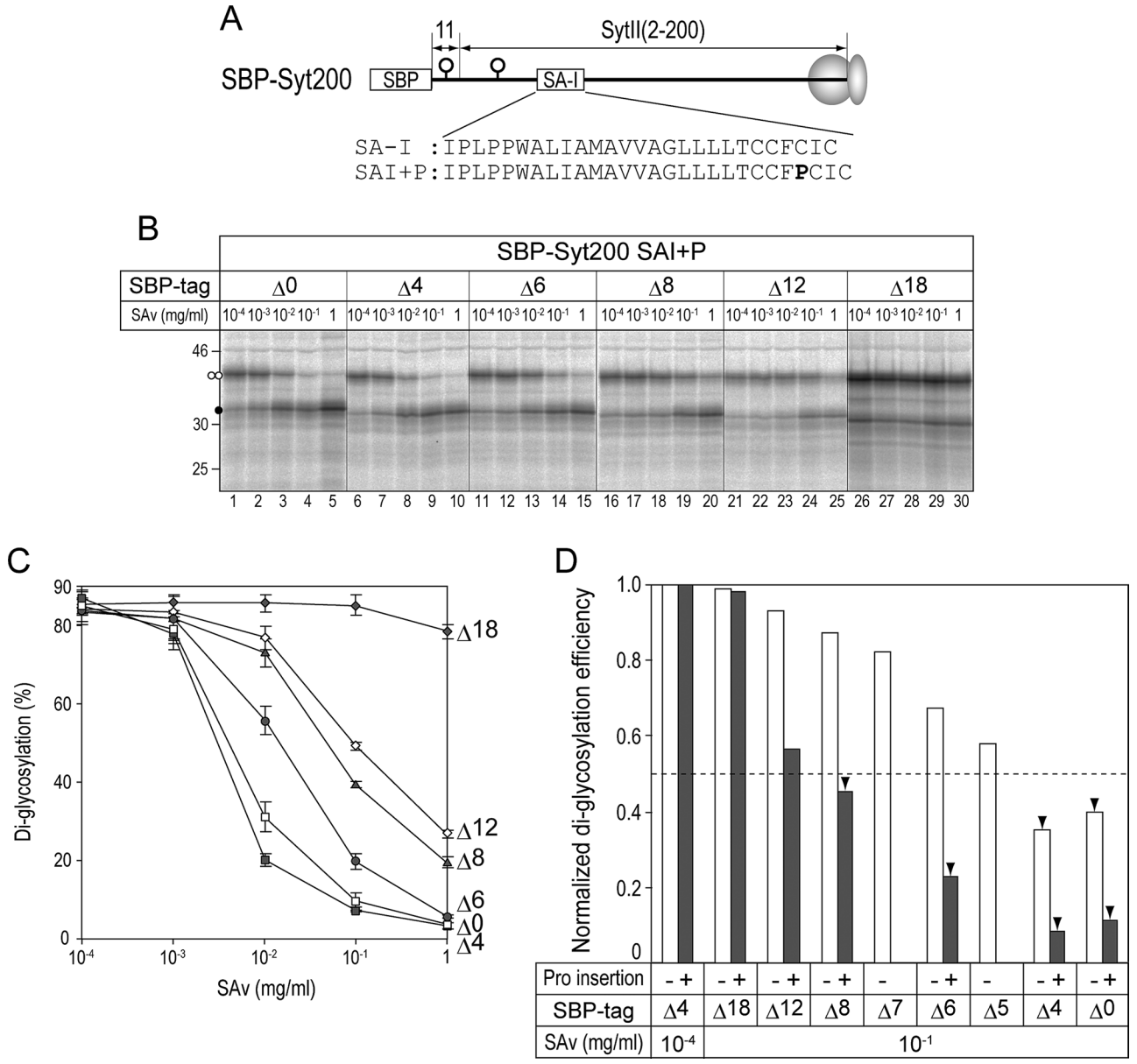

FIGURE 2: Truncated SBP tags become effective for translocation trapping by mutation in the SA-I sequence. (A) A proline residue was inserted into the SA-I sequence of SBP-Syt200 proteins. (B) Each protein was expressed and analyzed as shown in Figure 1. (C) Diglycosylated efficiency of each lane in B was quantified. Mean value and SD of three independent experiments. (D) Translocation efficiencies in the presence of 0.1 mg/ml SAv were compared between proteins containing normal and Pro-inserted SA-I sequences. Original data are shown in C and in Figure 1C. Diglycosylation efficiency relative to that of SBPΔ4-Syt200 proteins in the presence of 0.1 mg/ml SAv, which had maximal glycosylation efficiency in this study.

Several lumenal loops of the band 3 protein are translocated by the following SA-I–like TM sequence

Topogenic properties of TM sequences of human erythrocyte band 3 protein, which is believed to contain 13 TM sequences (Kanki *et al.*, 2002; Alper, 2006), were previously determined (Ota *et al.*, 1998a,b). These reports indicated that TM1 shows activity to start the transfer of its following part into the lumen, and TM2 possesses a stop-transfer function. Of interest, TM3, TM5, and TM7 possess only a weak start-transfer function, whereas TM4, TM6, and TM8 display topogenic properties like those of the SA-I sequence. Therefore a forced TM insertion model was proposed in which such internal SA-I–like TM sequences support membrane insertion of their upstream TM sequences by pulling into the translocon. This model provides the possibility that the upstream TM sequence and lumenal loop are temporally stalled on the cytosolic side. To examine this, we introduced an SBP tag and flanking N-glycosylation site (Figure 4A, G^{tag}), which is used as an indicator for translocation of the loop into the lumen, into all lumenal loops and one cytosolic loop between the TM1 and TM8 of the band 3 protein as shown in Figure 4A. Because glycosylation efficiency of the site can be influenced by distance from TM sequences (Nilsson and von Heijne, 1993), loop 3 was lengthened by insertion of original loop 3 sequence (Figure 4A, loop 3L). The band 3 protein possesses an endogenous N-glycosylation site at loop 7 (Figure 4A, G^{endo}), and

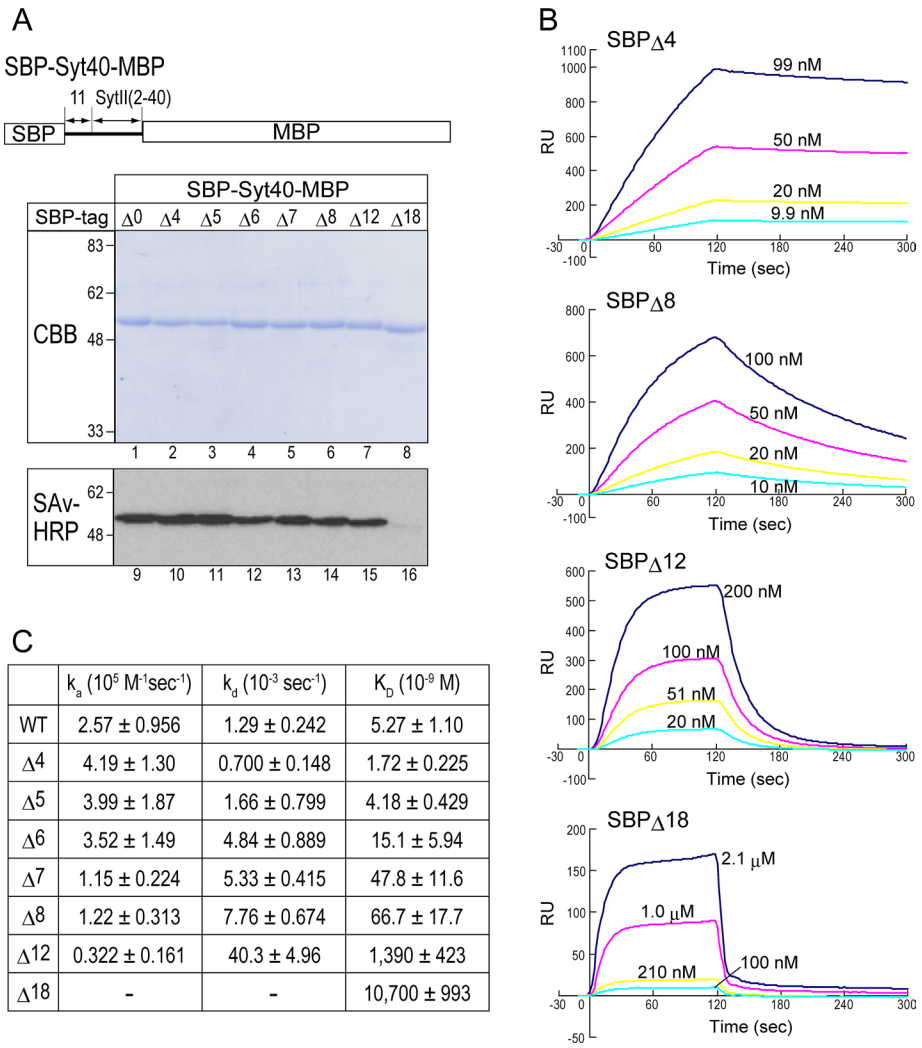

C

	k_a (10^5 $M^{-1}sec^{-1}$)	k_d (10^{-3} sec^{-1})	K_D (10^{-9} M)
WT	2.57 ± 0.956	1.29 ± 0.242	5.27 ± 1.10
Δ4	4.19 ± 1.30	0.700 ± 0.148	1.72 ± 0.225
Δ5	3.99 ± 1.87	1.66 ± 0.799	4.18 ± 0.429
Δ6	3.52 ± 1.49	4.84 ± 0.889	15.1 ± 5.94
Δ7	1.15 ± 0.224	5.33 ± 0.415	47.8 ± 11.6
Δ8	1.22 ± 0.313	7.76 ± 0.674	66.7 ± 17.7
Δ12	0.322 ± 0.161	40.3 ± 4.96	1,390 ± 423
Δ18	-	-	10,700 ± 993

FIGURE 3: SPR analysis of the interaction of normal and truncated SBP tags with streptavidin. (A) SBP-Syt40-MBP fusion proteins were expressed and purified. A 0.5-μg amount of each protein was analyzed by SDS–PAGE and visualized with Coomassie brilliant blue staining (middle). In addition, 0.1 μg of protein was detected by far-Western blotting using streptavidin–HRP conjugate (bottom). (B) Streptavidin was immobilized on a sensor chip in the measuring cell. The indicated concentrations of each SBP-Syt-MBP proteins were passed over the chip for 2 min and followed by running buffer. Association and dissociation kinetics were recorded. Several sets of sensorgrams are presented. (C) The k_a, k_d, and K_D values were obtained by the kinetics analysis method using BIAevaluation software, whereas the SBPΔ18 tag showed rather low affinity, and only its K_D value was calculated with the affinity analysis method of the software. Mean value and SD of three independent experiments.

thus proteins untagged and SBP tagged at cytosolic loop 6 were detected as monoglycosylated forms after cell-free synthesis in the presence of RM (Figure 4B, lanes 2 and 22). The glycosylation efficiency of the wild type was >80% (Figure 4C), indicating that the band 3 protein was efficiently targeted and integrated into the ER membrane in our cell-free system. On the other hand, proteins possessing an SBP tag in the lumenal loops were monoglycosylated and diglycosylated in the presence of RM (Figure 4B, lanes 7, 12, 17, and 27). In comparison with the efficiency of each glycosylation site (Figure 4D), the diglycosylation efficiency was almost equivalent to glycosylation at the G^{tag} site of each tagged loop (Figure 4C), whereas the glycosylation efficiency of tagged loop 1 was nearly equivalent to the sum of diglycosylated and G^{tag}-sole-glycosylated efficiencies. Glycosylation of G^{tag} sites was less efficient than that of the wild-type protein, and glycosylation at the G^{endo} site also was decreased by SBP tagging (Figure 4, C and D). Although we did not check the original translocation efficiency of each lumenal loop, insertion of the SBP tag and/or the flanking glycosylation site might influence translocation of the tagged loop and the following regions. In the presence of streptavidin, glycosylation of the protein tagged at loop 1 was not affected (Figure 4, B, lane 8, C, and D), indicating that this loop was not captured by cytosolic streptavidin. It must thus be translocated directly through the ribosome and translocon after start transfer by TM1. Glycosylation of SBP-tagged loops 3L, 5, and 7, however, was reduced in the presence of streptavidin (Figure 4, B–D), suggesting that these loops were exposed from the ribosome–translocon junction and could be captured with cytosolic streptavidin before translocation into the lumen. In addition, after incubation for 60 min in the presence of biotin, which removes streptavidin from the SBP tag, glycosylation of loops 5 and 7 was slightly improved (Figure 4B, lanes 19 and 29), indicating that some of these loops were in a translocation-competent state when they were trapped.

Among tagged lumenal loops, the translocation of loop 5 was most influenced by streptavidin. To further analyze this translocation, we partially deleted the SBP tag inserted in loop 5 (Figure 5A). In the absence of streptavidin, all proteins possessing normal and deleted tags at loop 5 were similarly monoglycosylated and diglycosylated (Figure 5B). In the presence of streptavidin, the translocation of loop 5 with the normal tag was considerably inhibited and the loop with six-residue-deleted tag was moderately trapped. Further, deleted tags showed little effect of the translocation arrest by streptavidin. Although the situation differs from that of the N-terminal portion of the SA-I sequence, trapping with a strong interaction is also required for the arrest of loop 5.

Moreover, to determine whether the translocation of loop 5 is caused by the following TM sequence, a proline residue, by which the topogenesis of the SA-I sequence was diminished (Figure 2), was also inserted into the TM6 (Figure 5A). When a proline residue was inserted between last two residues of TM6, the translocation of loop 5 was reduced independently of streptavidin (Figure 5C), whereas this is a position-dependent effect, and the proline residue at the one-upstream position did not influence the translocation. The proline residue can be detected in TM sequences (Yohannan *et al.*, 2004) in spite of its unfavorable property for the TM helix (Hessa *et al.*, 2005, 2007), and thus the influence of proline insertion might depend on the properties of the TM sequence and environment of inserted positions. Nevertheless, the properties of TM6 are crucial to the translocation of loop 5. If TM5 is a canonical start-transfer sequence, the translocation of loop 5

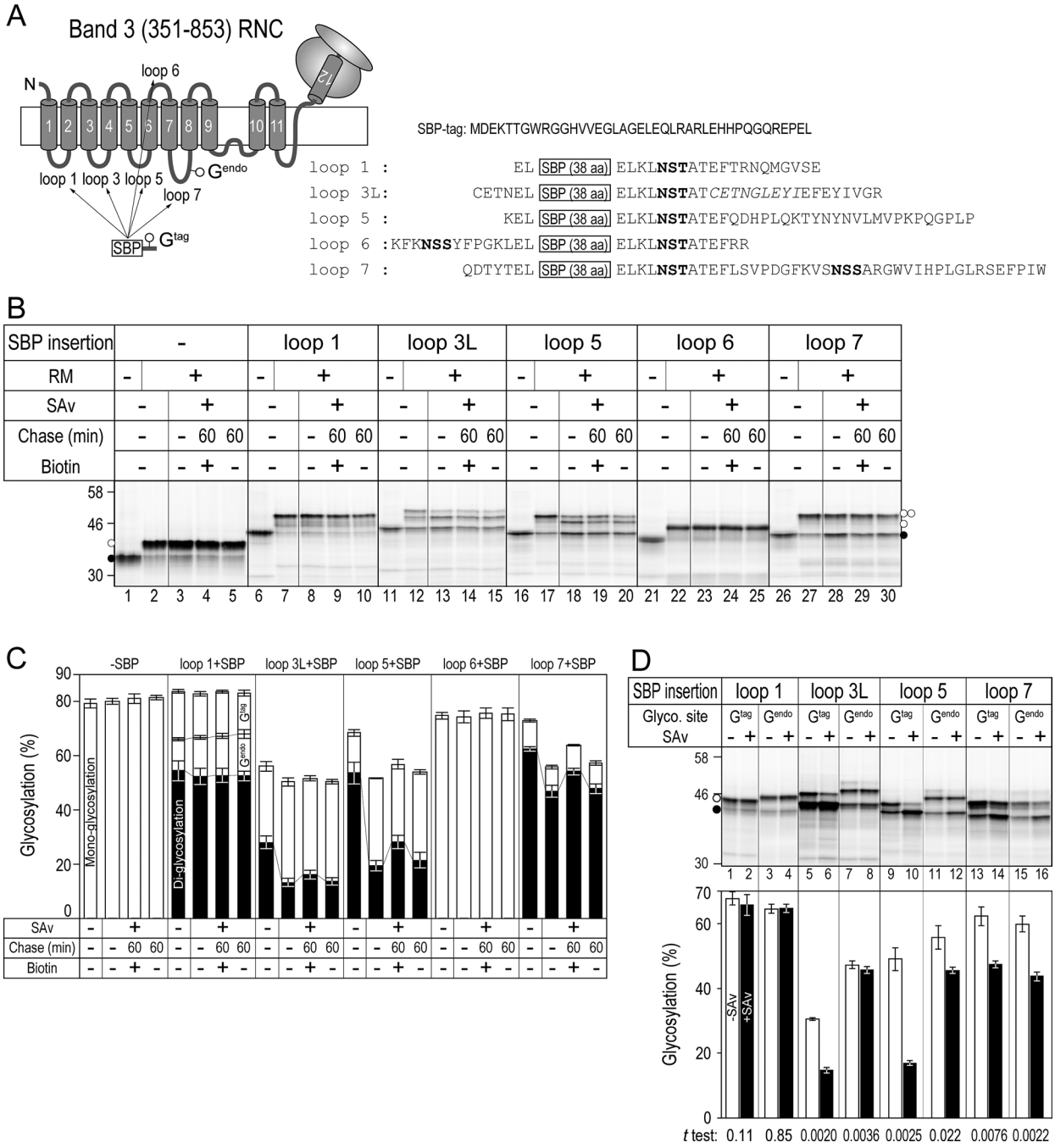

FIGURE 4: Several lumenal loops of the band 3 protein stalled on the cytoplasmic side before translocation. (A) The SBP tag and N-glycosylation probe sequence (G^{tag}; open circle) were inserted into the indicated loops of band 3. Open circle at loop 7 indicates an endogenous N-glycosylation site (G^{endo}). SBP-tag position and glycosylation-potential sites (bold letters) in each loop sequence. Because glycosylation efficiency of the site can be influenced by distance from TM sequences, loop 3 was lengthened (loop 3L) by insertion of original loop 3 sequence (italic letters). Truncated mRNAs coding Ala-352–Thr-853 of band 3 proteins (and initial Met) were used for in vitro translation. (B) Nascent chains of the band 3 containing or not containing SBP tag were synthesized in vitro in the presence (+) or absence (–) of RM and 1 mg/ml SAv. Where indicated, translation was terminated by cycloheximide, and translocation was further chased in the presence or absence of biotin for 60 min. Expressed proteins were analyzed as shown in Figure 1. (C) Quantification of B. Open and closed columns indicate monoglycosylated and diglycosylated efficiency, respectively. Diglycosylation efficiencies are equivalent to the glycosylation efficiencies of SBP-tagged loops. Mean value and SD of three independent experiments. (D) The glycosylation of each site of protein species with tagged loops (loop1, 3L, 5, and 7) was individually detected by silencing the other site. RM-supplemented cell-free synthesis in the absence or presence of SAv and analysis of the proteins were performed as in B. Glycosylation efficiency of each protein was quantified, and mean value and SD of three independent experiments are shown. Paired *t* test between the data sets in the absence and presence of SAv was also performed and reveals a significant difference ($p < 0.05$) between the data, except for the protein construct with tagged loop 1 (lanes 1–4).

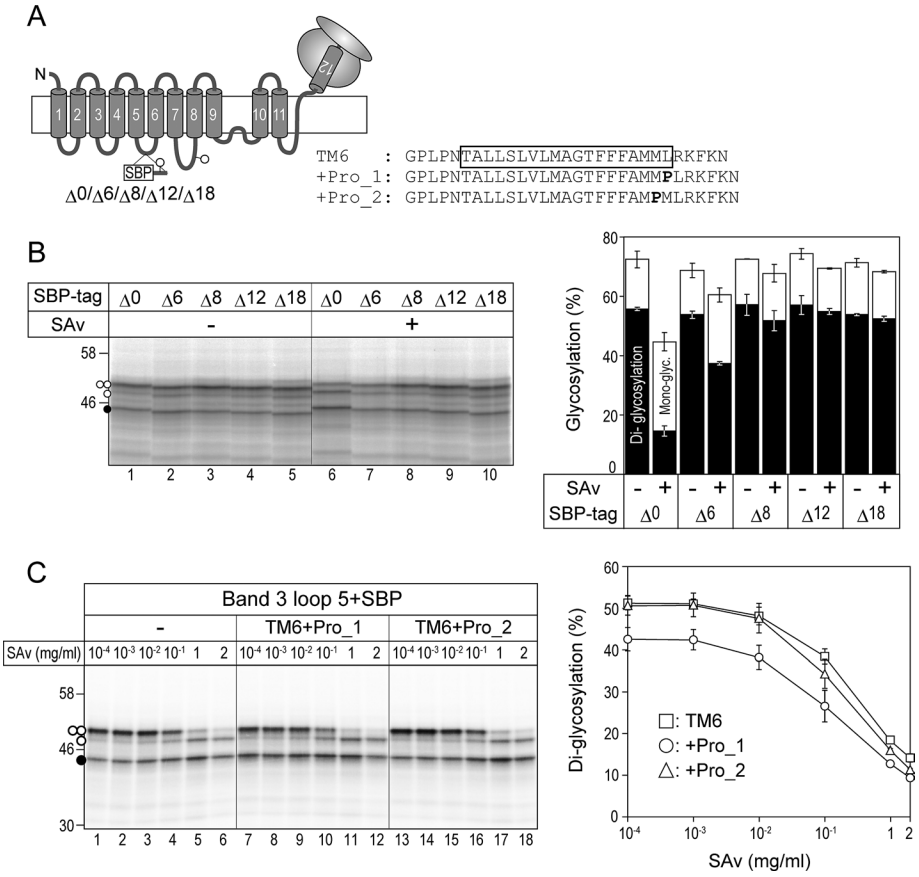

FIGURE 5: Translocation of the lumenal domain powered by the following TM sequence in a multispanning membrane protein. (A) Constructs used in this figure. For experiment B, the SBP tag inserted in loop 5 was deleted as shown in Figure 1. For experiment C, a proline residue was inserted into TM6 as shown. (B) Proteins containing full or truncated SBP tags in loop 5 were expressed in an RM-supplemented cell-free system in the presence or absence of 1 mg/ml SAv. Monoglycosylation and diglycosylation efficiencies were quantified. Mean value and SD of three independent experiments. (C) Proline insertion into TM6 diminishes translocation of the upstream loop 5. Those proteins were expressed in the presence of RM and indicated concentrations of SAv. Diglycosylation efficiencies were quantified. Mean value and SD of three independent experiments.

would be unrelated to the properties of TM6, and the mutation of TM6 should not cause the translocation defect. It is thus suggested that TM6 has a critical role in the translocation of loop 5.

The foregoing findings indicate that several lumenal loops in the band 3 protein can be stalled on the cytoplasmic side before their translocation and the translocation of at least one of these loops is mediated by the following TM sequence. This suggests that forced TM formation by internal SA-I–like TM sequences actually functions in the integration of the multispanning membrane protein.

Upstream translocation impairment is not critical to translocation of downstream parts

Although the translocation of the SBP tagged loop 5 decreases in the presence of streptavidin, monoglycosylated forms, which are glycosylated at the endogenous site only, increase under the same condition (Figures 4B and 6B). In addition, Figure 4D shows that the streptavidin-caused translocation impairment of the tagged loop 5 is ~32% (lanes 9 and 10), whereas that of loop 7 is only 10% (lanes 11 and 12). To examine the influence of the translocation impairment for translocation of the farther-downstream region, an N-glycosylation sequence derived from loop 7 (Figure 6A, Gloop) was introduced into loop 9, and the endogenous site at loop7 was simultaneously silenced. A new glycosylation site at loop 9 was efficiently glycosylated >80% in the absence of streptavidin, even when loop 5 or 7 was SBP tagged (Figure 6, B, lanes 8 and 11, and C, total glycosylation efficiencies). The translocation of loop 5 was similarly inhibited in the presence of streptavidin, whereas total glycosylation efficiency was still 70% (Figure 6, B, lanes 8 and 9, C), indicating that loop 9 can be translocated almost irrespectively of the translocation state of loop 5. These findings indicate that the translocation arrest of the upstream portion influences the translocation of the downstream parts, but the effect is regional. It is thus suggested that integration of TM sequences can be nearly independent of the integration states of their upstream parts and the translocon may be a flexible channel to accommodate a complex situation.

DISCUSSION

The present study investigated the translocation of lumenal domains of membrane proteins using SBP tagging. Translocation of the SBP-tagged N-terminal domain of the SA-I sequence into the ER lumen was trapped by streptavidin on the cytoplasmic side. Truncated SBP tags became ineffective in translocation arrest (Figure 1), whereas such tags with weaker abilities were sufficient for trapping the topogenesis of a proline-inserted SA-I sequence (Figure 2). Based on SPR analyses between truncated tags and streptavidin, an interaction as strong as 10^{-8} M or a smaller K_D is required for the translocation trapping of the protein species with the original SA-I sequence, and the affinity required for the translocation trapping depends on the primary structure of the SA-I sequence. We also analyzed the translocation of lumenal loops of an authentic multispanning membrane protein, band 3, by the same tagging method and found that several tagged lumenal loops could be trapped by streptavidin in the cytosol (Figure 4). The translocation of loop 5, which is a capturable lumenal loop, was diminished by proline insertion into the following TM6 with an $N_{lumen}/C_{cytosol}$ orientation (Figure 5), suggesting that this lumenal loop was not translocated after the start transfer of the upstream TM sequence, but instead by the following SA-I–like TM sequence. Moreover, the translocation arrest of an SBP-tagged loop only slightly affected the integration of subsequent parts (Figure 6), indicating that such TM sequences can be integrated almost independently of integration states of their upstream parts.

The trapping abilities of the truncated tags were well correlated with their affinity parameters to streptavidin, especially the values of the dissociation rate constant (Figure 3C). These parameters may represent the sum of local movements on the topogenesis of the SA-I sequence, such as insertion into the translocon and partitioning to the membrane, fluctuation of the translocating N-terminal domain, and its exposure from the ribosome–translocon junction to

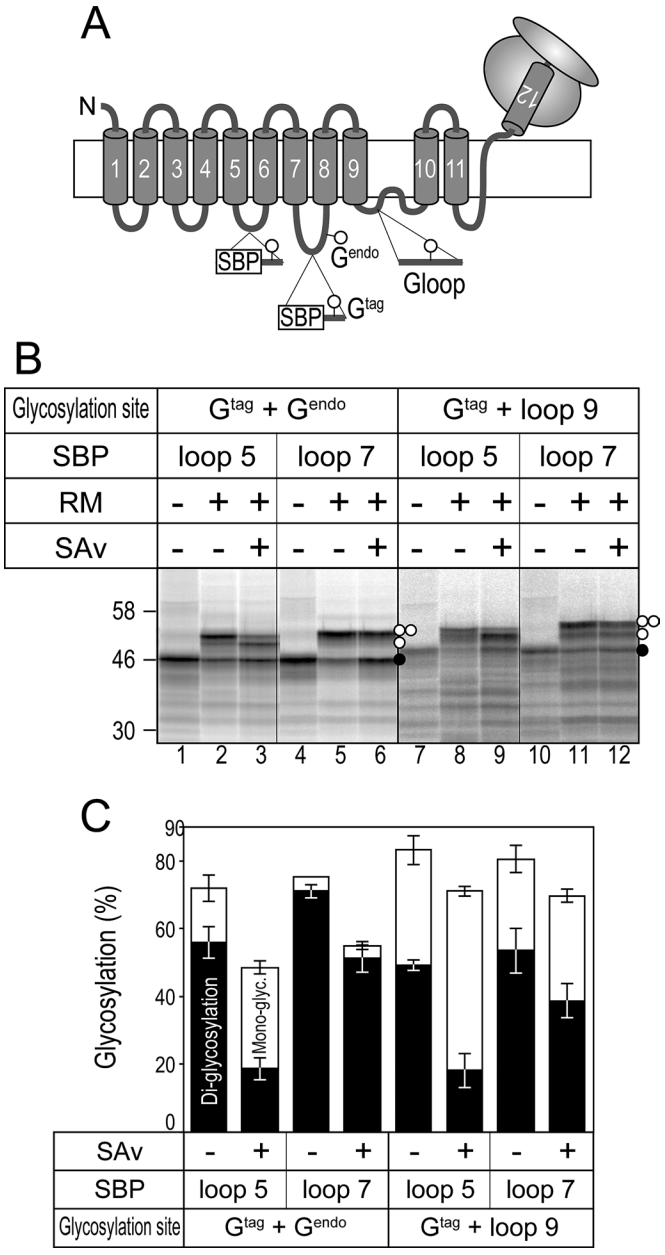

FIGURE 6: Influence of the translocation arrest on integration of the subsequent part. (A) To examine the effect on the translocation of loop 9 by the translocation trapping of loop 5 or 7, a glycosylation sequence derived from loop 7 (Gloop) was inserted into loop 9. To avoid complexity of multiple glycosylated forms, the endogenous glycosylation site in the protein species with glycosylation site–containing loop 9 was silenced. (B) Band 3 proteins were synthesized in vitro in the presence (+) or absence (–) of RM and 1 mg/ml SAv. (C) Quantification of B. Mean value and SD of three independent experiments.

the cytoplasm. Because mutation of the SA-I sequence diminished the affinity required for trapping, movement of the SA-I sequence must be one of the factors responsible for the motivation of the topogenesis. This finding is consistent with our previous reports, in which its hydrophobic core sequence is crucial for the translocation of N-terminally fused titin's immunoglobulin-like domain and SBP tag (Kida *et al.*, 2009), and a mutated SA-I sequence also shortens its membrane-embedded region (Kida *et al.*, 2010). Direct detection of movements of the translocon and polypeptide chains translocating and/or integrating via the translocon is difficult with the present technologies, and our data reveal one view of the actual movements of such events; more detailed and extensive analyses are required for understanding these movements.

Several studies reported that low topogenic and/or marginally hydrophobic TM sequences in multispanning membrane proteins are pulled and integrated into the membrane by the following flanking TM sequences possessing high topogenic functions (Lu *et al.*, 1998; Ota *et al.*, 1998b; Ojemalm *et al.*, 2012). Ota *et al.* (1998a) showed that isolated TM4, TM6, and TM8 possess an SA-I-like topogenic function. Our data reveal the temporal stall of several lumenal loops of the band 3 protein before translocation into the lumen. In addition, translocation of a lumenal loop was influenced by the primary structure of the following TM sequence. These findings suggest that translocation of lumenal loops powered by the following SA-I-like TM sequence actually functions in the integration of the multispanning membrane protein. Nevertheless, we cannot exclude other possibilities, including that two interacting TM sequences are inserted into the membrane or that such lumenal loops are stalled because the upstream TM sequences slowly start translocation of the following regions. Further exploration is required for clarification.

In our model case, two TM sequences should be simultaneously inserted into the membrane. Both TM sequences could be held in the Sec61 channel(s), or the following powering TM sequence could be partitioned into the lipid bilayer as soon as it enters the translocon and then the upstream TM sequence could be in the Sec61 channel. In addition, we found that TM9 could be integrated independently of the translocation impairment of loop 5. This provides the possibility that the translocon accommodates the arrested chain and the following TM sequence simultaneously by the functioning of two and more Sec61 channels. How such topogenesis is arranged by the translocon, however, remains to be elucidated.

Our results also indicate that the folding of multispanning membrane proteins can be manipulated by tagging and trapping the appropriate lumenal loops. Although reorientation of TM sequences of a membrane protein during integration has been reported (Lu *et al.*, 2000), removing fully integrated TM sequences from the membrane is difficult, and translocating intermediates of lumenal loops can be performed more easily by the technique used in this study. The selection of inserted tags is important. The SBP tag used in the present study possesses high affinity to streptavidin but inhibits translocation independently of streptavidin. In this case, the translocation of tagged loops by biotin is resumed to only a small extent. The remaining part without arrested TM sequences might be folded into a semistable state, or flanking TM sequences around the arrested portion might leave the translocon, but using a smaller tag at an appropriate position might become more efficient for resuming translocation. Although further improvement is required, our methodology might be useful for exploring the folding and structural reorganization of membrane proteins.

MATERIALS AND METHODS

Constructs

The plasmid used for the expression of SBP-Syt200 protein consisted of the SBP tag (MDEKTTGWRGGHVVEGLAGELEQLRARLEHHPQGQREP; each letter indicates 1 of 20 naturally occurring amino acid residues), a glycosylation probe sequence (KLNSTAT), and Arg-2–Arg-200 of mouse synaptotagmin II (SytII; an AflII site was generated just downstream of Arg-200 for synthesis of truncated mRNAs), as described previously (Kida *et al.*, 2007). DNA fragments coding fusion proteins of deleted SBP tags and SytII (Figure 1) were

obtained by PCR and introduced between the *Hin*dIII and *Xba*I sites of the pRc/CMV vector (Invitrogen, Carlsbad, CA). In Figure 2, a proline residue was inserted into the SA-I sequence by site-directed mutagenesis using Kunkel's method (Kunkel, 1985). To construct plasmids for the expression of SBP-Syt-MBP proteins, DNA fragments coding full and truncated SBP tags, a glycosylation probe sequence, SytII(2–40), and MBP were inserted between *Nco*I and *Xho*I sites of the pET15b vector (Novagen, Gibbstown, NJ). For synthesis in vitro, the TM domain of human band 3 (Met + Ala-352–Val-911) was introduced downstream of the *Xenopus* β-globin 5′-untranslated region in the pSP64T vector (Siegel and Walter, 1988). Two codons in each loop of band 3 were substituted for the *Eco*RI site, and the SBP tag and glycosylation probe sequence were introduced at the site of each loop as shown in Figure 4A. To further separate the glycosylation site from the TM4, loop 3 was lengthened by insertion of the original loop 3 sequence (C^{479}ETNGLEYI^{487}) as shown in Figure 4A by mutagenesis based on inverse PCR. In addition, in Figure 4D each glycosylation site of protein species was individually silenced by site-directed mutagenesis using the QuikChange procedure. In Figure 5, the SBP tag in loop 5 was deleted by inverse PCR-derived mutagenesis (sequences of deleted tags are shown in Figure 1A). In addition, a proline residue was introduced by a QuikChange procedure as shown in Figure 5A. To detect the translocation of loop 9 (Figure 6), two codons in loop 9 were substituted with the PmaCI site, the sequence coding a part of loop 7 (T^{627}YTQKLSVPDGFKVSNSSARGWVIHPLGLRSEFPIW^{662}) was introduced at the site, and endogenous glycosylation site in original loop 7 was simultaneously silenced by a QuikChange procedure. Sequences of all constructs were confirmed with DNA sequencing. Information for all of the oligo DNAs used in this study is available from the authors.

In vitro transcription, translation, and SDS–PAGE

For synthesis of truncated mRNAs coding SBP-Syt200 and its derivatives, plasmids were linearized by AflII at Arg-200 of SytII. For truncated mRNAs coding the band 3 transmembrane domain and its derivatives, plasmids were linearized by *Nae*I at Thr-853 (just after TM12). Template DNAs were transcribed with T7 RNA polymerase or SP6 RNA polymerase (Takara, Otsu, Japan) as previously described (Sakaguchi *et al*., 1992). mRNAs were translated in a reticulocyte lysate cell-free system for 1 h at 25°C in the absence or presence of RM. Preparation of RM (Walter and Blobel, 1983) and rabbit reticulocyte lysate (Jackson and Hunt, 1983) was performed as previously described. RM was extracted with EDTA and treated with *Staphylococcus aureus* nuclease (Roche, Indianapolis, IN) as described previously (Walter and Blobel, 1983). The translation reaction contained 32% reticulocyte lysate, 100 mM potassium acetate (KOAc), 1.0 mM magnesium acetate ($Mg(OAc)_2$), 20 kBq/μl EXPRESS protein-labeling mix (PerkinElmer, Waltham, MA), and 20 μg/ml castanospermine (Merck, Darmstadt, Germany) to inhibit the trimming of N-glycans in the ER lumen to simplify the mobility of N-glycosylated proteins on SDS–PAGE. Where indicated, 1 mg/ml or the indicated concentration of streptavidin (Wako, Osaka, Japan) was included in the translation reaction. For the translocation chase in the presence of biotin (Sigma-Aldrich, St. Louis, MO), translation was terminated by incubation in the presence of 2 mM cycloheximide (Sigma-Aldrich) for 10 min at 25°C and then further incubation at 25°C for 1 h in the presence of 0.4 mM biotin. After translation or the following chase incubation, samples were diluted with a 10-fold volume of dilution buffer (30 mM 4-(2-hydroxyethyl)-1-piperazineethanesulfonic acid [HEPES]/KOH, pH 7.4, 150 mM KOAc, 2 mM $Mg(OAc)_2$, 1 mM dithiothreitol) and centrifuged at 100,000 × *g* for 5 min at 4°C. ER-targeted radiolabeled proteins within the sedimented RM were analyzed by SDS–PAGE and visualized on a Bioimage Analyzer BAS-1800 (FujiFilm, Tokyo, Japan) or Typhoon FLA 7000 (GE Healthcare, Piscataway, NJ). Quantification was performed using Image Gauge, version 4.0 FujiFilm), or ImageQuant TL, version 7.0 (GE Healthcare), software.

Expression and purification of SBP-Syt-MBP proteins

Series of SBP-Syt-MBP fusion proteins were expressed in *E. coli* BL21(DE3) strain. After cell sonication, cell extracts were applied to an amylose resin (New England BioLabs, Ipswich, MA) column, and proteins bound to the resin were eluted with 10 mM maltose solution. Proteins were further purified by a size-exclusion column chromatography of Superdex 200 (GE Healthcare). Protein purity was checked by SDS–PAGE and Coomassie brilliant blue staining. These proteins were also detected by far-Western blotting using streptavidin–HRP conjugate (GE Healthcare).

SPR analysis of the interaction between SBP-Syt-MBP proteins and streptavidin

SPR analyses were performed at room temperature on a Biacore J system (GE Healthcare). Streptavidin was covalently conjugated to a carboxymethyl dextran–coated gold surface (sensor chip CM5; GE Healthcare), using an amide coupling kit according to the manufacturer's instructions. Next streptavidin was immobilized at a level of 5000 resonance units (RU). SBP-Syt-MBP proteins were diluted to indicated concentrations with HBS-EP buffer (10 mM HEPES, pH 7.4, 150 mM NaCl, 3 mM EDTA, 0.005% [vol/vol] Surfactant P20; GE Healthcare), and association and dissociation were monitored at a flow rate of 30 μl/min. To reuse the streptavidin-conjugated sensor chip, proteins associated on the chip were removed by 10 mM glycine/HCl, pH 2.2. The SPR signal was normalized using a reference flow cell containing no streptavidin and analyzed by BIAevaluation software (GE Healthcare). Values of K_D, k_a, and k_d were obtained by the kinetics analysis procedure of the software, whereas the SBPΔ18 tag showed rather low affinity, and only its K_D value was calculated with the affinity analysis procedure of the software. For each fusion protein, three independent experiments were performed, and the obtained values were averaged.

ACKNOWLEDGMENTS

This work was supported by Grants-in-Aid for Scientific Research from the Ministry of Education, Culture, Sports, Science, and Technology of Japan; the Global COE program; the Sumitomo Foundation; and the Hyogo Science and Technology Association.

REFERENCES

Alder NN, Johnson AE (2004). Cotranslational membrane protein biogenesis at the endoplasmic reticulum. J Biol Chem 279, 22787–22790.

Alper SL (2006). Molecular physiology of SLC4 anion exchangers. Exp Physiol 91, 153–161.

Do H, Falcone D, Lin J, Andrews DW, Johnson AE (1996). The cotranslational integration of membrane proteins into the phospholipid bilayer is a multistep process. Cell 85, 369–378.

Goder V, Spiess M (2001). Topogenesis of membrane proteins: determinants and dynamics. FEBS Lett 504, 87–93.

Heinrich SU, Mothes W, Brunner J, Rapoport TA (2000). The Sec61p complex mediates the integration of a membrane protein by allowing lipid partitioning of the transmembrane domain. Cell 102, 233–244.

Heinrich SU, Rapoport TA (2003). Cooperation of transmembrane segments during the integration of a double-spanning protein into the ER membrane. EMBO J 22, 3654–3663.

Hessa T, Kim H, Bihlmaier K, Lundin C, Boekel J, Andersson H, Nilsson I, White SH, von Heijne G (2005). Recognition of transmembrane helices by the endoplasmic reticulum translocon. Nature 433, 377–381.

Hessa T, Meindl-Beinker NM, Bernsel A, Kim H, Sato Y, Lerch-Bader M, Nilsson I, White SH, von Heijne G (2007). Molecular code for

transmembrane-helix recognition by the Sec61 translocon. Nature 450, 1026–1030.
Ismail N, Crawshaw SG, High S (2006). Active and passive displacement of transmembrane domains both occur during opsin biogenesis at the Sec61 translocon. J Cell Sci 119, 2826–2836.
Jackson RJ, Hunt T (1983). Preparation and use of nuclease-treated rabbit reticulocyte lysates for the translation of eukaryotic messenger RNA. Methods Enzymol 96, 50–74.
Kanki T, Sakaguchi M, Kitamura A, Sato T, Mihara K, Hamasaki N (2002). The tenth membrane region of band 3 is initially exposed to the luminal side of the endoplasmic reticulum and then integrated into a partially folded band 3 intermediate. Biochemistry 41, 13973–13981.
Kida Y, Kume C, Hirano M, Sakaguchi M (2010). Environmental transition of signal-anchor sequences during membrane insertion via the endoplasmic reticulum translocon. Mol Biol Cell 21, 418–429.
Kida Y, Morimoto F, Mihara K, Sakaguchi M (2006). Function of positive charges following signal-anchor sequences during translocation of the N-terminal domain. J Biol Chem 281, 1152–1158.
Kida Y, Morimoto F, Sakaguchi M (2007). Two translocating hydrophilic segments of a nascent chain span the ER membrane during multispanning protein topogenesis. J Cell Biol 179, 1441–1452.
Kida Y, Morimoto F, Sakaguchi M (2009). Signal anchor sequence provides motive force for polypeptide chain translocation through the endoplasmic reticulum membrane. J Biol Chem 284, 2861–2866.
Kida Y, Sakaguchi M, Fukuda M, Mikoshiba K, Mihara K (2000). Membrane topogenesis of a type I signal-anchor protein, mouse synaptotagmin II, on the endoplasmic reticulum. J Cell Biol 150, 719–730.
Kunkel TA (1985). The mutational specificity of DNA polymerase-beta during in vitro DNA synthesis. Production of frameshift, base substitution, and deletion mutations. J Biol Chem 260, 5787–5796.
Lu Y, Turnbull IR, Bragin A, Carveth K, Verkman AS, Skach WR (2000). Reorientation of aquaporin-1 topology during maturation in the endoplasmic reticulum. Mol Biol Cell 11, 2973–2985.
Lu Y, Xiong X, Helm A, Kimani K, Bragin A, Skach WR (1998). Co- and post-translational translocation mechanisms direct cystic fibrosis transmembrane conductance regulator N terminus transmembrane assembly. J Biol Chem 273, 568–576.
Martoglio B, Hofmann MW, Brunner J, Dobberstein B (1995). The protein-conducting channel in the membrane of the endoplasmic reticulum is open laterally toward the lipid bilayer. Cell 81, 207–214.
Mothes W, Heinrich SU, Graf R, Nilsson I, von Heijne G, Brunner J, Rapoport TA (1997). Molecular mechanism of membrane protein integration into the endoplasmic reticulum. Cell 89, 523–533.
Mothes W, Prehn S, Rapoport TA (1994). Systematic probing of the environment of a translocating secretory protein during translocation through the ER membrane. EMBO J 13, 3973–3982.
Nilsson IM, von Heijne G (1993). Determination of the distance between the oligosaccharyltransferase active site and the endoplasmic reticulum membrane. J Biol Chem 268, 5798–5801.
Ojemalm K, Halling KK, Nilsson I, von Heijne G (2012). Orientational preferences of neighboring helices can drive ER insertion of a marginally hydrophobic transmembrane helix. Mol Cell 45, 529–540.
Ota K, Sakaguchi M, Hamasaki N, Mihara K (1998a). Assessment of topogenic functions of anticipated transmembrane segments of human band 3. J Biol Chem 273, 28286–28291.
Ota K, Sakaguchi M, von Heijne G, Hamasaki N, Mihara K (1998b). Forced transmembrane orientation of hydrophilic polypeptide segments in multispanning membrane proteins. Mol Cell 2, 495–503.
Park E, Rapoport TA (2012). Mechanisms of Sec61/SecY-mediated protein translocation across membranes. Annu Rev Biophys 41, 21–40.
Plath K, Mothes W, Wilkinson BM, Stirling CJ, Rapoport TA (1998). Signal sequence recognition in posttranslational protein transport across the yeast ER membrane. Cell 94, 795–807.
Sadlish H, Pitonzo D, Johnson AE, Skach WR (2005). Sequential triage of transmembrane segments by Sec61alpha during biogenesis of a native multispanning membrane protein. Nat Struct Mol Biol 12, 870–878.
Sakaguchi M (1997). Eukaryotic protein secretion. Curr Opin Biotechnol 8, 595–601.
Sakaguchi M, Tomiyoshi R, Kuroiwa T, Mihara K, Omura T (1992). Functions of signal and signal-anchor sequences are determined by the balance between the hydrophobic segment and the N-terminal charge. Proc Natl Acad Sci USA 89, 16–19.
Shao S, Hegde RS (2011). Membrane protein insertion at the endoplasmic reticulum. Annu Rev Cell Dev Biol 27, 25–56.
Siegel V, Walter P (1988). Each of the activities of signal recognition particle (SRP) is contained within a distinct domain: analysis of biochemical mutants of SRP. Cell 52, 39–49.
Tsukazaki T *et al.* (2008). Conformational transition of Sec machinery inferred from bacterial SecYE structures. Nature 455, 988–991.
Van den Berg B, Clemons WM Jr, Collinson I, Modis Y, Hartmann E, Harrison SC, Rapoport TA (2004). X-ray structure of a protein-conducting channel. Nature 427, 36–44.
Walter P, Blobel G (1983). Preparation of microsomal membranes for cotranslational protein translocation. Methods Enzymol 96, 84–93.
Wilson DS, Keefe AD, Szostak JW (2001). The use of mRNA display to select high-affinity protein-binding peptides. Proc Natl Acad Sci USA 98, 3750–3755.
Yohannan S, Faham S, Yang D, Whitelegge JP, Bowie JU (2004). The evolution of transmembrane helix kinks and the structural diversity of G protein-coupled receptors. Proc Natl Acad Sci USA 101, 959–963.